

Rejuvenating image-GPT as Strong Visual Representation Learners

Sucheng Ren^{1*} Zeyu Wang^{2*} Hongru Zhu¹ Junfei Xiao¹ Alan Yuille¹ Cihang Xie²

*equal contribution

¹ Johns Hopkins University ² UC Santa Cruz

Abstract

This paper enhances image-GPT (iGPT), one of the pioneering works that introduce autoregressive pretraining to predict next pixels for visual representation learning. Two simple yet essential changes are made. First, we shift the prediction target from raw pixels to semantic tokens, enabling a higher-level understanding of visual content. Second, we supplement the autoregressive modeling by instructing the model to predict not only the next tokens but also the visible tokens. This pipeline is particularly effective when semantic tokens are encoded by discriminatively trained models, such as CLIP. We introduce this novel approach as D-iGPT. Extensive experiments showcase that D-iGPT excels as a strong learner of visual representations: A notable achievement of D-iGPT is its compelling performance on the ImageNet-1K dataset — by training on publicly available datasets, D-iGPT achieves 89.5% top-1 accuracy with a vanilla ViT-Large model. This model also shows strong generalization on the downstream task and robustness on out-of-distribution samples. Code is available at <https://github.com/OliverRensu/D-iGPT>.

1. Introduction

The advent of Large Language Models (LLMs) [31, 44, 46], such as the GPT series [4, 31, 34], has catalyzed a transformative era in natural language processing (NLP), establishing new precedents for performance across a range of linguistic tasks. One of the key driving forces behind this tremendous success is autoregressive pretraining, which trains models to predict the most probable next tokens in a sequence. This foundational strategy enables the models to internalize a complex interplay of syntax and semantics, which in turn translates to their extraordinary prowess to process language with human-like capabilities.

Beyond NLP, autoregressive pretraining has also been a significant contributor in the field of computer vision. The pioneering model in this context is PixelCNN [48], a deep autoregressive model designed to model the discrete proba-

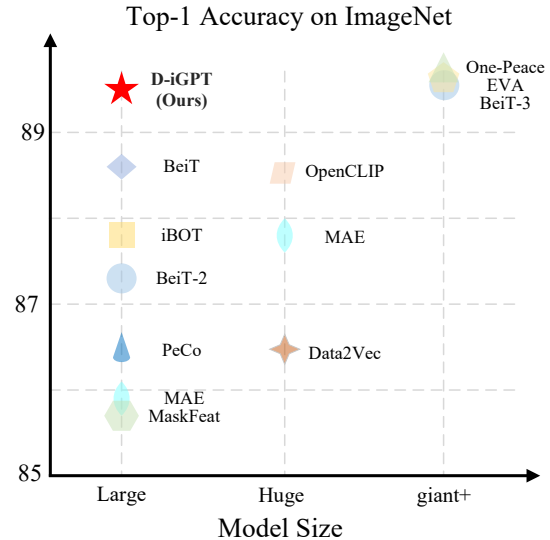


Figure 1. ImageNet performance of models trained on publicly available datasets. We note D-iGPT achieves competitive performance with a vanilla ViT-L model.

bility of the raw pixel values and encode the complete set of dependencies in the image. Building upon this foundation, image GPT (iGPT) [6] represents a significant advancement, tilizing the flexible Transformer architecture [49] at a notably larger computational scale. iGPT’s achievements are remarkable: it not only learned state-of-the-art visual representation for lower-resolution datasets such as CIFAR-10 but also demonstrated competitive performance on more complex datasets like ImageNet.

Despite the initial successes of autoregressive pretraining in computer vision, recent trends have witnessed a rapid paradigm shift towards BERT-style pretraining [14]. This transition is significant, particularly when considering iGPT’s initial findings of comparable performance between autoregressive and BERT-style pretraining in various tasks. Subsequent research, however, has increasingly favored BERT-style pretraining [2, 19] for its superior efficacy in visual representation learning. For example, MAE [19] demonstrates that simply predicting the values of randomly masked pixels can effectively serve as a scalable solution for visual representation learning.

In this paper, we revisit iGPT, challenging that *autoregressive pretraining is actually capable of building strong vision learners, especially at scale*. Our methodology incorporates two critical modifications. First, acknowledging that images are inherently noisy and redundant, we follow BEiT [2] to “tokenize” images into semantic tokens. This adjustment reorients the autoregressive prediction focus from pixels to semantic tokens, thereby enabling a more nuanced understanding of the interplay among different image regions. Second, we complement the generative decoder, which is responsible for autoregressively predicting the next semantic token, with a discriminative decoder. This additional component is tasked with predicting the semantic tokens of the visible pixels. Moreover, an intriguing observation is that this pretraining pipeline works best when the semantic visual tokens are derived from models trained discriminatively, such as CLIP [35]. We term this enhanced approach as D-iGPT.

Extensive experiments across various datasets and tasks confirm the effectiveness of our proposed D-iGPT. With ImageNet-1K as the sole pertaining dataset, our base-size model achieves an 86.2% top-1 classification accuracy, surpassing previous state-of-the-art by 0.6%. Additionally, with 36 million publicly available datasets, our large-size model achieves an 89.5% top-1 classification accuracy. With much less training data and smaller model size, D-iGPT performs similarly to previous state-of-the-arts trained on public datasets. We also evaluate D-iGPT on semantic segmentation and it outperforms MAE counterparts using the same pretraining and finetuning dataset.

2. Related Work

2.1. Self-supervised Learning

According to learning targets, self-supervised learning methods can be broadly grouped into discriminative-based and generative-based.

Discriminative Self-supervised Learning. This paradigm focuses on learning transferable representation by defining a pre-task that scores the discriminative power of learned representations. A notable strategy within this category is contrastive learning, which utilizes a contrastive loss to learn representation similarity or dissimilarity between the same images with different augmentation or entirely different images. For instance, Wu *et al.* [55] introduces instance discrimination, constructing positive and negative query-key pairs from the same or different images. SimCLR [7] further improves the performance with a projection head, strong data augmentations, and large-batch-size training. MoCo [8, 18] incorporates memory bank and late weight updates without the need for large batch sizes. CLIP [35] extends this concept by incorporating natural language supervision through image-text pairings.

Generative Self-supervised Learning. In contrast to the discriminative approaches, generative self-supervised learning emphasizes training models to reconstruct the original inputs from corrupted versions. Masked image modeling, inspired by BERT [14] in NLP, is the dominant strategy in this line of research. For example, the pioneering work BEiT [2] pretrains models to recover the original visual tokens based on the corrupted image patches. Other significant methods include MAE [19], SimMIM [57], MaskFeat [53], PeCo [15], MILAN [24], DeepMIM [37].

This study pivots towards a distinct facet of generative self-supervised learning, namely, autoregressive pretraining. In NLP, autoregressive pretraining is also highly regarded alongside BERT-style methods, especially effective in the era of LLMs [31, 46]. However, its progress in computer vision has not yet paralleled the heightened interest sparked by the initial success of iGPT [6]. This paper aims to bridge this gap. We demonstrate that, with simple yet essential modification, autoregressive pretraining exhibits excellent capabilities in building strong vision models.

2.2. ImageNet-1K Winning Solutions

The advancements in ImageNet-1K performance have seen a significant boost, primarily driven by scaling datasets and model sizes. Liu *et al.* [29] exemplify this trend with the successful training of SwinV2-G, a model equipped with 3.0 billion parameters, using techniques like residual-post-norm and scaled cosine attention. Similarly, Dehghani *et al.* [13] have shown the impressive capabilities of ViT-22B, highlighting the feasibility of “LLM-like” scaling in computer vision. Zhang *et al.* [60] investigate scaling both model and data, providing valuable insights into the interplay between scaling factors and performance. Another noteworthy development is by Chen *et al.* [9] which discovers deep neural network training algorithms through program search, leading to the creation of the effective and memory-efficient optimizer Lion. However, a common limitation across these methods is their heavy reliance on private, in-house data, such as JFT-3B [60], which raises significant reproducibility concerns.

In contrast to the approaches above, there is a notable trend of employing public datasets to train more powerful vision models. For instance, Wang *et al.* [52] scale BEiT-3 to 1.9 billion parameters using a combination of images, texts, and image-text pairs, all sourced from public datasets. Likewise, Fang *et al.* [17] successfully scaled up EVA, a vanilla ViT with 1.0 billion parameters, using a total of 29.6 million public images. One-Peace [51] presents a 4-billion-parameter model capable of unifying vision, audio, and language representations. Our D-iGPT model stands out in this landscape by achieving superior performance to EVA with a smaller model size and paralleling the performance of One-Peace with significantly smaller model and data sizes.

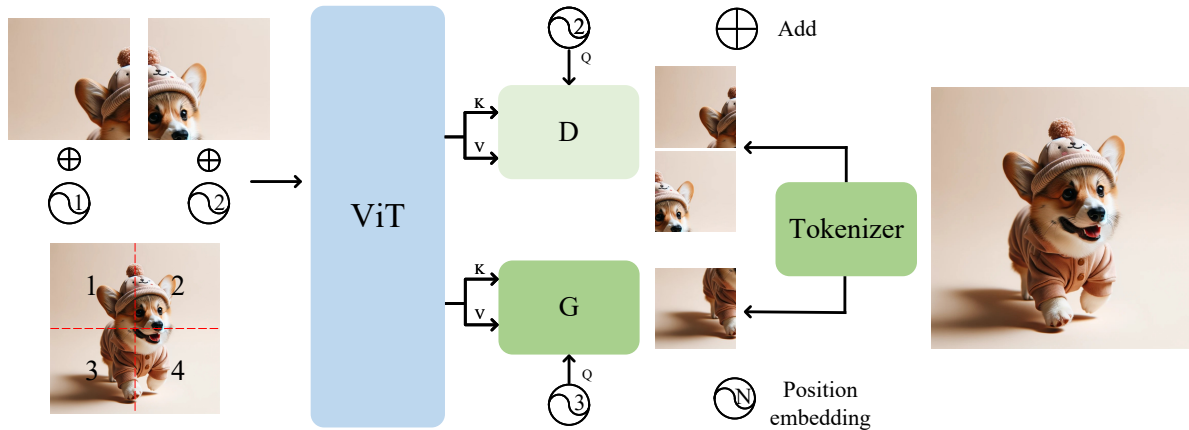


Figure 2. The overview illustration of D-iGPT.

3. Method

We hereby first revisit iGPT in Section 3.1. Next, we present our enhanced version, D-iGPT, in Section 3.2, which shifts the prediction target from raw pixels to semantic tokens and additionally supplies supervision on visible tokens. Lastly, the specifics of our model’s architecture, along with implementation details, are elaborately discussed in Section 3.3.

3.1. Revisiting iGPT

GPT. In NLP, the generative pretraining involves modeling the probability of the next word in a corpus $\mathcal{U} = \{u_1, \dots, u_n\}$ autoregressively. This can be written as:

$$p(u) = \prod_{i=1}^n p(u_i | u_1, \dots, u_{i-1}, \Theta) \quad (1)$$

Here, GPT computes the likelihood of each word u_i based on the context of all preceding words from u_1 to u_{i-1} , aiming to minimize the negative log-likelihood of the target words:

$$\mathcal{L} = -\log p(u) \quad (2)$$

Image GPT. In the context of images, where the input is an image $X \in \mathcal{R}^{H \times W \times C}$, the challenge lies in converting this 2D structure into a sequential format akin to a language sequence. iGPT [6] addresses this by naïvely vectorizing the image X into a series of individual pixels $\{x_1, \dots, x_n\}$, treating each pixel as analogous to a word. It then models the probability of each subsequent pixel based on the preceding ones in the sequence:

$$p(x) = \prod_{i=1}^n p(x_i | x_1, \dots, x_{i-1}, \Theta) \quad (3)$$

In this formulation, iGPT aims to predict each pixel x_i utilizing the information from preceding pixels $\{x_1, \dots, x_{i-1}\}$,

minimizing the negative log-likelihood:

$$\mathcal{L} = -\log p(x) \quad (4)$$

Nevertheless, the extensive computational demands of iGPT, primarily due to the quadratic complexity of attention mechanisms relative to sequence length, limit its applicability for various vision tasks. For iGPT, this sequence length corresponds to the total number of pixels $Seq = H \times W$. As such, iGPT is primarily suited for low-resolution images (e.g., $Seq = 32 \times 32$).

To mitigate this computational challenge, especially for high-resolution image training, approaches like SAIM [33] and RandSac [26] have been developed. A critical advancement in these methodologies is the incorporation of the Vision Transformer (ViT) architecture [16], which significantly transforms the approach to tokenization — instead of treating each pixel as an individual token, ViT redefines tokens as image patches (e.g., clusters of pixels). This strategy effectively reduces the sequence length for each image, thereby enabling the practical application of iGPT to higher-resolution images.

3.2. D-iGPT

Our development of D-iGPT is built upon the iGPT with the ViT architecture. Additionally, unlike iGPT completely drops the knowledge of the 2D input structure, D-iGPT is designed to carefully encode this information. This encoding is crucial for facilitating a more intricate interplay between different regions of an image, thereby enhancing the effectiveness of autoregressive modeling. Specifically, at the input level, images are divided into multiple equally-sized, non-overlapping patches, forming clusters $S = \{s_1, \dots, s_n\}$. Each cluster serves as a fundamental unit in the sequence for autoregressive modeling, e.g., each s in iGPT is a single pixel. Consequently, the autoregressive probability, previously defined for individual pixels in iGPT

(as in Equation 3), is now reformulated for these clusters as:

$$p(s) = \prod_{i=1}^n p(s_i | s_1, \dots, s_{i-1}, \Theta) \quad (5)$$

By default, we configure the cluster size to 4, corresponding to a dimension of 112×112 for an input image of 224×224 , as illustrated in Figure 2.

Building upon this new setup, we next introduce two simple yet essential modifications to enhance iGPT.

Modification I: semantic tokens. In contrast to the inherently semantically-rich nature of text, raw pixels in images generally lack such depth of meaning. Addressing this semantic discrepancy is crucial for enhancing learning efficacy in models like iGPT. To bridge this gap, our approach, inspired by BEiT [2], involves transitioning the autoregressive target of D-iGPT from raw pixels to semantic tokens, which can be written as:

$$\mathcal{L}_G = - \sum_{i=1}^n \text{cosine}(G(f(x_{s_1:s_{i-1}}); \theta_G), f_\phi(x)_{s_i}), \quad (6)$$

where $f(\cdot)$ is the encoder, $f_\phi(x)_{s_i}$ is the semantically enriched tokens corresponding to the cluster s_i , and $G(\cdot; \theta_G)$ is the generative decoder for autoregressive prediction. Furthermore, to break the dependency on a fixed sequence order and enhance learning flexibility, we adopt strategies from [25, 58] by randomly permuting the sequence of clusters $\{s_1, \dots, s_n\}$ and selecting a permutation π .

Modification II: supervision on visible clusters. To further enhance the training of our model, we introduce additional supervision targeting visible clusters. This is formulated as:

$$\mathcal{L}_D = - \sum_{i=1}^n \text{cosine}(D(f(x_{s_1:s_{i-1}}); \theta_D), f_\phi(x)_{s_1:s_{i-1}}) \quad (7)$$

where $D(\cdot; \theta_D)$ is the discriminative decoder, tasked with predicting the semantic tokens of visible pixels.

This approach, as encapsulated in Equation (7), can be conceptualized as a form of knowledge distillation. The objective is to enable the encoder of D-iGPT (the student model) to distill knowledge from the model $f_\phi(x)$ (the teacher model), which provides semantic tokens, based on the visible sequence of clusters $\{s_1, \dots, s_{i-1}\}$. However, our methodology differs from traditional knowledge distillation frameworks [23, 54], which typically align logits or feature maps between teacher and student models directly. Instead, we incorporate a discriminative decoder $D(\cdot; \theta_D)$ to disentangle this knowledge distillation supervision from the original autoregressive supervision (carried out via the generative decoder $G(\cdot; \theta_G)$). This design is crucial for ensuring the acquisition of high-quality representations, as demonstrated in the subsequent experimental section.

Summary. The integration of these two modifications significantly enhances the capabilities of iGPT for visual representation learning. While there are various options for the model $f_\phi(x)$ to generate semantic tokens, our empirical findings, as detailed next, indicate a marked preference for discriminatively trained models like CLIP [35].

Moreover, from an implementation perspective, we adopt the attention mask strategy as employed in [6, 26, 31, 34]. This approach facilitates efficient computation of input sequences of varying lengths (e.g., a set of input sequences such as $\{\{s_1\}, \{s_1, s_2\}, \dots, \{s_1, s_2, \dots, s_{n-1}\}\}$) within a single iteration. We direct interested readers to the supplementary materials for more details.

3.3. Architecture

The D-iGPT architecture is composed of two primary components: the encoder and the decoder. For the encoder, it leverages the standard ViT architecture. For the decoders, we incorporate several Transformer decoder blocks. Note that D-iGPT utilizes two distinct types of decoders: the discriminative decoder D for discriminative training, and the generative decoder G for generative pretraining. Although these decoders share an identical architectural framework, they are characterized by different sets of parameters. As shown in Figure 2, they take the randomly initialized [Dis] tokens D or [Gen] tokens G with position information as the query, and the output features from the encoder as the key and the value:

$$\begin{aligned} \hat{D}_{l+1} &= \text{Atten}(D_l, h_L, h_L), \\ D_{l+1} &= \text{MLP}(\hat{D}_{l+1}), \\ \hat{G}_{l+1} &= \text{Atten}(G_l, h_L, h_L), \\ G_{l+1} &= \text{MLP}(\hat{G}_{l+1}), \end{aligned} \quad (8)$$

where $\text{Atten}(q, k, v)$ represents the cross-attention mechanism with Query (q), Key (k), and Value (v), and h_L denotes the output features from the encoder. Notably, in downstream tasks, we utilize only the encoder, discarding the decoder component.

4. Experiment

Implementation details. In our experiments, we use CLIP for providing semantic tokens. We pretrain, by default, all models on ImageNet-1K for 300 epochs. We set the batch size to 4096 and the peak learning rate to $lr = 1.5e^{-4} \times \text{batchsize}/256$. We adopt a cosine learning rate decay schedule with a warm-up period of 40 epochs, and utilize the AdamW [30] optimizer with a weight decay of 0.05. We use random resized cropping and random horizontal flipping, with the input size set to 224×224 .

When extending pretraining to ImageNet-21K, all models undergo 150 epochs of pretraining with a warm-up pe-

Method	Pretraining Epochs	Tokenizer/Teacher	Classification (top-1 %)	Segmentation (mIoU)
<i>Base-size models (ViT-B)</i>				
DeiT [45]	300	Label	81.2	47.2
SdAE [10]	300	EMA	84.1	48.6
PeCo [15]	300	VQGAN	84.1	46.7
TinyMIM [38]	300	MAE	85.0	52.2
FD [54]	300	CLIP	84.8	-
BEiTv2 [32]	300	CLIP+VQGAN	85.0	52.7
BEiT [2]	800	DALLE	84.0	-
MAE [19]	1600	Pixel	83.6	48.1
Randsac [26]	1600	Pixel	83.7	-
PeCo [15]	800	VQGAN	84.5	48.5
data2vec [1]	800	EMA	84.2	-
SIM [43]	1600	EMA	83.8	-
iBOT [62]	1600	EMA	84.0	-
MaskFeat [53]	1600	HOG	84.0	-
BEiTv2 [32]	1600	CLIP+VQGAN	85.5	53.1
DeepMIM [37]	1600	CLIP	85.6	53.1
MILAN [24]	1600	CLIP	85.6	-
EVA [17]	800	CLIP	85.5	53.3
D-iGPT (Ours)	300	CLIP	86.2	53.8
<i>Large-size models (ViT-L)</i>				
BEiTv2 [32]	300	CLIP+VQGAN	86.6	55.0
BEiT [2]	800	DALLE	85.2	-
MAE [19]	1600	Pixel	85.9	53.6
PeCo [15]	800	VQGAN	86.5	-
iBOT [62]	1600	EMA	84.8	-
MaskFeat [53]	1600	HOG	85.7	-
BEiTv2 [32]	1600	CLIP+VQGAN	87.3	56.7
MILAN [24]	1600	CLIP	86.8†	-
D-iGPT (Ours)	300	CLIP	87.8	57.3

Table 1. Fine-tuning results which methods were pretrained on **ImageNet-1K** and fine-tuned on ImageNet-1K/CoCo/ADE20K on classification, detection, and semantic segmentation. †: reproduced result using official code.

riod of 5 epochs, learning rate $lr = 1.5e^{-3}$, and batch size of 4096. Additionally, for models pretrained on merged publicly available datasets as described in [17], all models are pretrained for 60 epochs with a warm-up period of 2 epochs, learning rate $lr = 1.5e^{-3}$, and batch size of 4096.

4.1. ImageNet-1K Pretraining

For a fair comparison with previous work [1, 2, 15, 19, 32, 37, 38, 53], we first study pretraining on ImageNet-1K [39] dataset with ViT-B/16 and ViT-L.

4.1.1 ImageNet Classification

Following [19, 38], we finetune pretrained models using the ImageNet-1K training dataset, and test it on the ImageNet-1K validation dataset with the input size of 224×224 .

Note that different from previous approaches such as [59, 60], which employs multi-head attention pooling, and

BEiT-3 [52], which exploits an additional pretrained giant language tower as the image classification task layer, we hereby opt for a simple linear layer for classification. We finetune the pretrained model for 100 epochs.

Results. As shown in Table 1, our ViT-B impressively achieves 86.2% top-1 accuracy. This is the first instance of a ViT-B model surpassing the 86% accuracy threshold on ImageNet-1K, using an input size of 224×224 .

In terms of comparative performance, D-iGPT demonstrates a significant improvement over various existing methods. It exceeds the baseline supervised model, DeiT, by a substantial margin of **+5.0%**, the prevalent mask image modeling method, MAE, by **+2.6%**, and the prior art MILAN/DeepMIM by **+0.6%**. Furthermore, with the same teacher model, D-iGPT surpasses EVA by **+0.7%**, while requiring only 37.5% of the training epochs.

When enlarging the model size to ViT-L size, our D-iGPT sets a new benchmark with an accuracy of 87.8%.

Method	ImageNet \uparrow	IN-V2 \uparrow	IN-Real \uparrow	IN-Adversarial \uparrow	IN-Rendition \uparrow	IN-Corruption \downarrow	IN-Sketch \uparrow
<i>Base-size models (ViT-B)</i>							
DeiT [45]	81.2	70.6	86.7	27.9	45.4	36.8	32.3
TinyMIM [38]	85.0	75.3	88.7	43.0	54.6	32.7	41.0
MAE [19]	83.6	72.9	88.1	33.6	50.0	37.8	36.4
BEiT [2]	83.2	71.8	87.9	32.8	49.6	38.7	35.1
iBOT [62]	84.0	73.0	88.2	33.0	51.2	36.9	38.7
BEiTv2 [32]	85.5	76.2	89.2	54.0	61.7	30.9	45.9
D-iGPT (Ours)	86.2	76.4	89.6	56.3	64.3	29.9	48.5
<i>Large-size models (ViT-L)</i>							
MAE [19]	85.9	76.5	89.4	56.3	61.0	31.1	45.6
BEiT [2]	85.2	75.1	88.8	55.4	59.8	32.0	43.8
iBOT [62]	84.8	74.4	87.9	53.9	57.1	34.1	42.6
BEiTv2 [32]	87.3	78.3	90.0	68.6	70.3	25.4	53.7
D-iGPT (Ours)	87.8	79.6	90.4	73.0	80.5	24.7	60.3

Table 2. Robustness and Generalization evaluation on out-of-domain datasets.

Notably, this result surpasses the well-known mask image modeling MAE by **+1.9%** and prior art BEiT-v2 by **+0.5%**.

4.1.2 Semantic Segmentation

For semantic segmentation, we evaluate D-iGPT using the ADE20K dataset [61], which comprises 150 categories with 20,000 training images and 2,000 validation images. Following MAE [19], we adopt our D-iGPT pretrained ViT model as the backbone and UperNet [56] as the framework. The input image resolution is 512×512 for training and evaluation; we report mIoU as the evaluation metric.

Table 1 reports the impressive performance of D-iGPT on ADE20K. For the ViT-B model, D-iGPT achieves a mIOU of 53.8, and for ViT-L, it reaches a mIOU of 57.3. These results set new benchmarks for their respective model sizes. For example, D-iGPT outperforms the closest competing solutions by margins of 0.5 in ViT-B and 0.6 in ViT-L. Such performance highlights the strong generalization capabilities of D-iGPT on downstream tasks.

4.1.3 Robustness

We next assess model robustness on various out-of-domain ImageNet datasets, including natural adversarial examples (ImageNet-A [22]), semantic shifts (ImageNet-R [21]), common image corruptions (ImageNet-C [20]), image sketches (ImageNet-S [50]), ImageNet-V2 [36], and ImageNet-Real [3].

As indicated in Table 2, D-iGPT consistently outperforms both supervised models like DeiT and self-supervised models like MAE across all datasets, showcasing notable improvements in robustness and generalization. For example, compared with the prior art BEiT-v2, D-iGPT exhibits superior robustness with improvements ranging from 0.2%

to 2.6% in the ViT-B model size category. These improvements are even more striking with the ViT-L model, *i.e.*, D-iGPT makes significant strides in challenging datasets like IN-Adversarial (improvement of +4.4%), IN-Sketch (+6.6%), and IN-Rendition (+10.2%).

4.2. Pretraining with Larger Datasets

We hereby explore the impact of pretraining on two extensive datasets: 1) ImageNet-21K with 14 million samples, and 2) ~ 36 million publicly available images, as employed in [17]. Following [2, 17], we initially undertake supervised fine-tuning on the ImageNet-21K training dataset for 60 epochs; subsequently, we finetune the D-iGPT model on the ImageNet-1K training dataset.

Main Results. The scaling results of D-iGPT, as depicted in Table 3, are particularly noteworthy. When pretrained with ImageNet-21k, the D-iGPT enhanced ViT-L model achieves a Top-1 accuracy of 89.5%. This performance not only parallels other baselines such as BEiT-3 and EVA but also is attained with a considerably smaller model and training data size. Notably, our D-iGPT is comparable to those achieved by substantially larger models that have been trained with extensive private datasets [9, 12, 28]. These results demonstrate the scalability and efficacy of D-iGPT for visual representation learning.

4.3. Zero-shot Classification

We finetune our D-iGPT on the vision-language dataset for zero-shot ImageNet classification. With such fine-tuning, our D-iGPT can be applied to a wide array of vision classification tasks directly with class names, without the need for task-specific fine-tuning. Additionally, the finetuned feature can be utilized in both uni-modal and multi-modal applications, including AI generation, akin to the capabilities demonstrated by CLIP features [35].

Method	Model	Model Size	Pretraining Data Category	Pretraining Data Size	ImageNet-1K top-1 (%)
TokenLearner [40]	TokenLearner	460M	I	300M (Private)	88.9
MaxViT [47]	MaxViT	475M	I	300M (Private)	89.5
SwinV2 [29]	SwinV2	3B	I	84M (Private)	90.2
CoAtNet-7 [12]	CoAtNet	2.44B	I	300M (Private)	90.9
Lion [9]	ViT	2.44B	I	3B (Private)	91.1
BEiT [2]	ViT	306M	I	14M	88.6
iBOT [62]	ViT	306M	I	14M	87.8
OpenClip-H [11]	ViT	632M	I-T	2B	88.5
BeiT-3 [52]	ViT	1B	I-T,I,T	21M,14M,160GB	89.6
EVA [17]	ViT	1B	I	30M	89.7
One-Peace [51]	Transformer	4B	I-T,A-T	2B,8k hours	89.8
D-iGPT-L (ours)	ViT	306M	I	14M	89.5

Table 3. Summary of D-iGPT on various vision benchmarks. I, T, and A indicate images, texts, and audios respectively. Method indicate using private training data.

Pretraining	Model	DataSet	Samples	top-1
CLIPA	ViT-L/16	LAION-400M	128M	69.3
D-iGPT	ViT-L/16	LAION-400M	128M	71.6
OpenClip	ViT-L/14	LAION-400M	1B	75.3
D-iGPT	ViT-L/14	LAION-400M	1B	77.1

Table 4. Zero-shot classification performance on ImageNet-1K. Samples indicate the seen samples in finetuning.

For this process, we use the D-iGPT pretrained image encoder and the OpenCLIP [11] pretrained text encoder as our starting point. The model is then fine-tuned on the LAION dataset [41, 42]. The results, as summarized in Table 4, showcase significant enhancements achieved by D-iGPT. For example, compared to CLIPA [27] and OpenClip, D-iGPT improves the zero-shot ImageNet classification accuracy by 2.3% and 1.8%, respectively.

4.4. Ablation Study

Semantic tokens. Our study begins with an examination of various semantic token sources. Beyond our chosen CLIP tokens and iGPT’s pixel-based tokens, we also consider alternatives like DINO features [5, 53] and VQVAE tokens [32]. The results, shown in Table 5, reveal notable differences in performance. While autoregressive pretraining using low-level pixels or VQVAE tokens shows lesser efficacy compared to MAE, the application of tokens from discriminatively trained models significantly enhances D-iGPT’s performance, surpassing MAE by a notable margin.

Given the superior performance achieved with CLIP features, we next delve deeper into the effects of utilizing tokens from different CLIP variants. As detailed in Table 6, when we use a larger tokenizer (CLIP-L), D-iGPT achieves better performance compared to using the smaller tokenizer (CLIP-B). However, if we employ CLIP-L@336 as the to-

Method	Tokenizer	ImageNet-1K top-1 Acc.	ADE20K mIoU
MAE [19]	Pixel	82.6	47.1
iGPT† [6]	Pixel	82.0	44.1
MAE [19]	VQVAE	82.2	46.8
D-iGPT	VQVAE	82.3	47.0
MAE [19]	DINO	84.0	50.1
D-iGPT	DINO	84.7	51.0
MAE [19]	CLIP	84.6	52.1
D-iGPT	CLIP	86.2	53.8

Table 5. Ablation on different semantic tokens. † indicates implement with the same architecture but different Tokenizers as our D-iGPT.

kenizer while maintaining the input size of 224×224 , the D-iGPT performance significantly drops, likely due to a resolution mismatch during the training and inference phases of CLIP-L@336.

Further experiments explore various large-size tokenizers including DINO, CLIP, and OpenCLIP. Using OpenCLIP-L as the tokenizer, which is similar to CLIP in approach but varies in training data, results in comparable performance to employing CLIP-L. An even larger tokenizer, OpenCLIP-H, further enhances D-iGPT’s performance. Conversely, tokenizers like DINO do not yield as favorable results. This suggests that larger pretraining datasets and the inclusion of textual information are likely beneficial in generating high-quality semantic tokens for guiding D-iGPT’s learning process.

Pretraining paradigm In our evaluation of various pretraining paradigms, we include Mask Image Modeling (MIM), Knowledge Distillation (KD), and our D-iGPT. To facilitate a fair comparison, especially for the MIM-based

Student	Tokenizer Source	ImageNet-1K top-1 Acc.	ADE20K mIoU
ViT-B	CLIP-B	85.7	53.0
ViT-B	CLIP-L	85.9	53.3
ViT-B	CLIP-L@336	84.6	51.8
ViT-B	DINO-L	84.8	52.0
ViT-B	CLIP-L	85.9	53.3
ViT-B	OpenCLIP-L	85.9	53.2
ViT-B	OpenCLIP-H	86.2	53.6

Table 6. Ablation on tokenizer model.

Method	ImageNet-1K top-1 Acc.	ADE20K mIoU
MAE† [19]	84.6	52.1
EVA [17]	85.0	52.6
KD [54]	85.0	52.5
D-iGPT	86.2	53.8

Table 7. Ablation on the pretraining paradigm. MAE† is the reproduced version by incorporating CLIP features as supervision targets

MAE model, we modify it to utilize CLIP features as the supervision target, moving away from the conventional pixel-based approach. The results are presented in Table 7.

The baseline pretraining methods, such as MAE, EVA, and KD, exhibit comparable performance levels in both ImageNet classification and ADE20K semantic segmentation tasks. However, our D-iGPT model achieves markedly better results. For instance, while the highest performance among baseline models on ImageNet is 85.0% accuracy and on ADE20K is 52.6 mIoU, D-iGPT significantly elevates these benchmarks to 86.2% accuracy on ImageNet and 53.8 mIoU on ADE20K. These findings underscore the potential of autoregressive pretraining, implemented in D-iGPT, as a more scalable and effective paradigm for visual representation learning.”

Decoder Design Our investigation begins with an examination of *Decoder Depth*. In this context, we compare our D-iGPT’s performance using a lightweight decoder against the 8-layer decoder found in the MAE model. Intriguingly, this simpler decoder architecture not only significantly reduces GPU computational load but also enhances overall performance. As shown in Table 8, a 2-layer decoder outperforms a 4-layer decoder, even when maintaining the same decoder dimension of 1024.

Building on the success of the 2-layer decoder, we next turn our attention to the *Decoder Dimension (Dim)*. Through our experiments, we note that a reduction in decoder dimension results in a slight decrease in model performance. This finding highlights the nuanced impact of

Dec. Depth	Dec. Dim	ImageNet-1K top-1 Acc.	ADE20K mIoU
1	1024	85.6	52.8
2	1024	86.2	53.6
4	1024	86.0	53.2
2	512	85.8	53.0
2	768	85.9	53.3
2	1024	86.2	53.6

Table 8. Ablation on the decoder design.

Method	Gen Decoder	Dis Decoder	ImageNet-1K (top-1 Acc.)
FD [54]			84.9
D-iGPT	✓		85.1
D-iGPT	✓	✓	86.2

Table 9. Ablation on the discriminative decoder.

decoder dimensionality on D-iGPT’s effectiveness.

Discriminative Decoder. In the D-iGPT architecture, we incorporate a discriminative decoder, specifically designed to separate the discriminative pretraining from the generative pretraining processes. To evaluate its effectiveness, we conducted an ablation study where we removed the discriminative pretraining and instead implemented feature distillation [54] directly on the output feature map of the encoder. The results of this study, as depicted in Table 9, reveal a notable insight. Applying feature distillation directly to the encoder’s features leads to a decrease of 1.1% in accuracy. This outcome underscores the critical role of the discriminative decoder in maintaining the efficacy and clarity of the pretraining process in our D-iGPT model.

5. Conclusion

In this work, we introduce D-iGPT, a novel adaptation of the iGPT model that transitions the focus of prediction from raw pixels to semantic tokens and supplements the supervision of visual pixels. This significant modification has led to a groundbreaking achievement: D-iGPT attains an impressive 89.5% top-1 accuracy on the ImageNet dataset, a feat accomplished using solely publicly available datasets. We hope our D-iGPT can inspire more research on rethinking autoregressive pretraining for visual representation learning and bring fresh perspectives on building vision foundation models on publicly available data sources.

Acknowledgment

This work is partially supported by TPU Research Cloud (TRC) program and Google Cloud Research Credits program.

References

- [1] Alexei Baevski, Wei-Ning Hsu, Qiantong Xu, Arun Babu, Jiatuo Gu, and Michael Auli. Data2vec: A general framework for self-supervised learning in speech, vision and language. *arXiv preprint arXiv:2202.03555*, 2022. **5**
- [2] Hangbo Bao, Li Dong, Songhao Piao, and Furu Wei. BEiT: BERT pre-training of image transformers. In *International Conference on Learning Representations*, 2022. **1, 2, 4, 5, 6, 7**
- [3] Lucas Beyer, Olivier J Hénaff, Alexander Kolesnikov, Xiaoohua Zhai, and Aäron van den Oord. Are we done with imagenet? *arXiv preprint arXiv:2006.07159*, 2020. **6**
- [4] Tom B. Brown, Benjamin Mann, Nick Ryder, Melanie Subbiah, Jared Kaplan, Prafulla Dhariwal, Arvind Neelakantan, Pranav Shyam, Girish Sastry, Amanda Askell, Sandhini Agarwal, Ariel Herbert-Voss, Gretchen Krueger, T. J. Henighan, Rewon Child, Aditya Ramesh, Daniel M. Ziegler, Jeff Wu, Clemens Winter, Christopher Hesse, Mark Chen, Eric Sigler, Matusz Litwin, Scott Gray, Benjamin Chess, Jack Clark, Christopher Berner, Sam McCandlish, Alec Radford, Ilya Sutskever, and Dario Amodei. Language models are few-shot learners. *ArXiv*, abs/2005.14165, 2020. **1**
- [5] Mathilde Caron, Hugo Touvron, Ishan Misra, Hervé Jégou, Julien Mairal, Piotr Bojanowski, and Armand Joulin. Emerging properties in self-supervised vision transformers. *arXiv preprint arXiv:2104.14294*, 2021. **7**
- [6] Mark Chen, Alec Radford, Rewon Child, Jeffrey Wu, Heewoo Jun, David Luan, and Ilya Sutskever. Generative pre-training from pixels. In *Proceedings of the 37th International Conference on Machine Learning*, pages 1691–1703. PMLR, 2020. **1, 2, 3, 4, 7**
- [7] Ting Chen, Simon Kornblith, Mohammad Norouzi, and Geoffrey Hinton. A simple framework for contrastive learning of visual representations. *preprint arXiv:2002.05709*, 2020. **2**
- [8] Xinlei Chen, Haoqi Fan, Ross Girshick, and Kaiming He. Improved baselines with momentum contrastive learning. *preprint arXiv:2003.04297*, 2020. **2**
- [9] Xiangning Chen, Chen Liang, Da Huang, Esteban Real, Kaiyuan Wang, Yao Liu, Hieu Pham, Xuanyi Dong, Thang Luong, Cho-Jui Hsieh, et al. Symbolic discovery of optimization algorithms. *arXiv preprint arXiv:2302.06675*, 2023. **2, 6, 7**
- [10] Yabo Chen, Yuchen Liu, Dongsheng Jiang, Xiaopeng Zhang, Wenrui Dai, Hongkai Xiong, and Qi Tian. Sdae: Self-distilled masked autoencoder. *ArXiv*, abs/2208.00449, 2022. **5**
- [11] Mehdi Cherti, Romain Beaumont, Ross Wightman, Mitchell Wortsman, Gabriel Ilharco, Cade Gordon, Christoph Schuhmann, Ludwig Schmidt, and Jenia Jitsev. Reproducible scaling laws for contrastive language-image learning. In *Proceedings of the IEEE/CVF Conference on Computer Vision and Pattern Recognition*, pages 2818–2829, 2023. **7**
- [12] Zihang Dai, Hanxiao Liu, Quoc V Le, and Mingxing Tan. Coatnet: Marrying convolution and attention for all data sizes. *Advances in neural information processing systems*, 34:3965–3977, 2021. **6, 7**
- [13] Mostafa Dehghani, Josip Djolonga, Basil Mustafa, Piotr Padlewski, Jonathan Heek, Justin Gilmer, Andreas Peter Steiner, Mathilde Caron, Robert Geirhos, Ibrahim Alabdulmohsin, et al. Scaling vision transformers to 22 billion parameters. In *International Conference on Machine Learning*, pages 7480–7512. PMLR, 2023. **2**
- [14] Jacob Devlin, Ming-Wei Chang, Kenton Lee, and Kristina Toutanova. BERT: pre-training of deep bidirectional transformers for language understanding. In *Proceedings of the 2019 Conference of the North American Chapter of the Association for Computational Linguistics: Human Language Technologies*, pages 4171–4186. Association for Computational Linguistics, 2019. **1, 2**
- [15] Xiaoyi Dong, Jianmin Bao, Ting Zhang, Dongdong Chen, Weiming Zhang, Lu Yuan, Dong Chen, Fang Wen, and Nenghai Yu. Peco: Perceptual codebook for bert pre-training of vision transformers. *arXiv preprint arXiv:2111.12710*, 2021. **2, 5**
- [16] Alexey Dosovitskiy, Lucas Beyer, Alexander Kolesnikov, Dirk Weissenborn, Xiaohua Zhai, Thomas Unterthiner, Mostafa Dehghani, Matthias Minderer, Georg Heigold, Sylvain Gelly, et al. An image is worth 16x16 words: Transformers for image recognition at scale. *preprint arXiv:2010.11929*, 2020. **3**
- [17] Yuxin Fang, Wen Wang, Binhui Xie, Quan Sun, Ledell Wu, Xinggang Wang, Tiejun Huang, Xinlong Wang, and Yue Cao. Eva: Exploring the limits of masked visual representation learning at scale. *arXiv preprint arXiv:2211.07636*, 2022. **2, 5, 6, 7, 8**
- [18] Kaiming He, Haoqi Fan, Yuxin Wu, Saining Xie, and Ross Girshick. Momentum contrast for unsupervised visual representation learning. In *CVPR*, 2020. **2**
- [19] Kaiming He, Xinlei Chen, Saining Xie, Yanghao Li, Piotr Dollár, and Ross Girshick. Masked autoencoders are scalable vision learners. In *CVPR*, 2022. **1, 2, 5, 6, 7, 8**
- [20] Dan Hendrycks and Thomas Dietterich. Benchmarking neural network robustness to common corruptions and perturbations. *ICLR*, 2019. **6**
- [21] Dan Hendrycks, Steven Basart, Norman Mu, Saurav Kadavath, Frank Wang, Evan Dorundo, Rahul Desai, Tyler Zhu, Samyak Parajuli, Mike Guo, Dawn Song, Jacob Steinhardt, and Justin Gilmer. The many faces of robustness: A critical analysis of out-of-distribution generalization. *ICCV*, 2021. **6**
- [22] Dan Hendrycks, Kevin Zhao, Steven Basart, Jacob Steinhardt, and Dawn Song. Natural adversarial examples. *CVPR*, 2021. **6**
- [23] Geoffrey Hinton, Oriol Vinyals, and Jeff Dean. Distilling the knowledge in a neural network. *arXiv preprint arXiv:1503.02531*, 2015. **4**
- [24] Zejiang Hou, Fei Sun, Yen-Kuang Chen, Yuan Xie, and S. Y. Kung. Milan: Masked image pretraining on language assisted representation. *ArXiv*, abs/2208.06049, 2022. **2, 5**
- [25] Tianyu Hua, Yonglong Tian, Sucheng Ren, Michalis Raptis, Hang Zhao, and Leonid Sigal. Self-supervision through random segments with autoregressive coding (randsac). In *The Eleventh International Conference on Learning Representations*, 2022. **4**

- [26] Tianyu Hua, Yonglong Tian, Sucheng Ren, Michalis Raptis, Hang Zhao, and Leonid Sigal. Self-supervision through random segments with autoregressive coding (randsac). In *The Eleventh International Conference on Learning Representations*, 2022. 3, 4, 5
- [27] Xianhang Li, Zeyu Wang, and Cihang Xie. An inverse scaling law for clip training. *arXiv preprint arXiv:2305.07017*, 2023. 7
- [28] Ze Liu, Han Hu, Yutong Lin, Zhuliang Yao, Zhenda Xie, Yixuan Wei, Jia Ning, Yue Cao, Zheng Zhang, Li Dong, Furu Wei, and Baining Guo. Swin transformer v2: Scaling up capacity and resolution. In *International Conference on Computer Vision and Pattern Recognition (CVPR)*, 2022. 6
- [29] Ze Liu, Han Hu, Yutong Lin, Zhuliang Yao, Zhenda Xie, Yixuan Wei, Jia Ning, Yue Cao, Zheng Zhang, Li Dong, et al. Swin transformer v2: Scaling up capacity and resolution. In *Proceedings of the IEEE/CVF conference on computer vision and pattern recognition*, pages 12009–12019, 2022. 2, 7
- [30] Ilya Loshchilov and Frank Hutter. Decoupled weight decay regularization. In *International Conference on Learning Representations*, 2019. 4
- [31] OpenAI. Gpt-4 technical report. *ArXiv*, abs/2303.08774, 2023. 1, 2, 4
- [32] Zhiliang Peng, Li Dong, Hangbo Bao, Qixiang Ye, and Furu Wei. BEiT v2: Masked image modeling with vector-quantized visual tokenizers. *arXiv preprint arXiv:2208.06366*, 2022. 5, 6, 7
- [33] Yu Qi, Fan Yang, Yousong Zhu, Yufei Liu, Liwei Wu, Rui Zhao, and Wei Li. Exploring stochastic autoregressive image modeling for visual representation. In *Proceedings of the AAAI Conference on Artificial Intelligence*, pages 2074–2081, 2023. 3
- [34] Alec Radford and Karthik Narasimhan. Improving language understanding by generative pre-training. 2018. 1, 4
- [35] Alec Radford, Jong Wook Kim, Chris Hallacy, Aditya Ramesh, Gabriel Goh, Sandhini Agarwal, Girish Sastry, Amanda Askell, Pamela Mishkin, Jack Clark, et al. Learning transferable visual models from natural language supervision. In *ICML*, pages 8748–8763. PMLR, 2021. 2, 4, 6
- [36] Benjamin Recht, Rebecca Roelofs, Ludwig Schmidt, and Vaishaal Shankar. Do imagenet classifiers generalize to imagenet? In *International conference on machine learning*, pages 5389–5400. PMLR, 2019. 6
- [37] Sucheng Ren, Fangyun Wei, Samuel Albanie, Zheng Zhang, and Han Hu. Deepmim: Deep supervision for masked image modeling. 2023. 2, 5
- [38] Sucheng Ren, Fangyun Wei, Zheng Zhang, and Han Hu. TinyMim: An empirical study of distilling mim pre-trained models. In *Proceedings of the IEEE/CVF Conference on Computer Vision and Pattern Recognition (CVPR)*, pages 3687–3697, 2023. 5, 6
- [39] Olga Russakovsky, Jia Deng, Hao Su, Jonathan Krause, Sanjeev Satheesh, Sean Ma, Zhiheng Huang, Andrej Karpathy, Aditya Khosla, Michael Bernstein, Alexander C Berg, and Li Fei-Fei. Imagenet large scale visual recognition challenge. *IJCV*, 2015. 5
- [40] Michael S Ryoo, AJ Piergiovanni, Anurag Arnab, Mostafa Dehghani, and Anelia Angelova. Tokenlearner: What can 8 learned tokens do for images and videos? *arXiv preprint arXiv:2106.11297*, 2021. 7
- [41] Christoph Schuhmann, Richard Vencu, Romain Beaumont, Robert Kaczmarczyk, Clayton Mullis, Aarush Katta, Theo Coombes, Jenia Jitsev, and Aran Komatsuzaki. Laion-400m: Open dataset of clip-filtered 400 million image-text pairs. *arXiv preprint arXiv:2111.02114*, 2021. 7
- [42] Christoph Schuhmann, Romain Beaumont, Richard Vencu, Cade Gordon, Ross Wightman, Mehdi Cherti, Theo Coombes, Aarush Katta, Clayton Mullis, Mitchell Wortsman, et al. Laion-5b: An open large-scale dataset for training next generation image-text models. *Advances in Neural Information Processing Systems*, 35:25278–25294, 2022. 7
- [43] Chenxin Tao, Xizhou Zhu, Gao Huang, Yu Qiao, Xiaogang Wang, and Jifeng Dai. Siamese image modeling for self-supervised vision representation learning. *arXiv preprint arXiv:2206.01204*, 2022. 5
- [44] Romal Thoppilan, Daniel De Freitas, Jamie Hall, Noam Shazeer, Apoorv Kulshreshtha, Heng-Tze Cheng, Alicia Jin, Taylor Bos, Leslie Baker, Yu Du, et al. Lambda: Language models for dialog applications. *arXiv preprint arXiv:2201.08239*, 2022. 1
- [45] Hugo Touvron, Matthieu Cord, Matthijs Douze, Francisco Massa, Alexandre Sablayrolles, and Hervé Jégou. Training data-efficient image transformers & distillation through attention. *preprint arXiv:2012.12877*, 2020. 5, 6
- [46] Hugo Touvron, Louis Martin, Kevin Stone, Peter Albert, Amjad Almahairi, Yasmine Babaei, Nikolay Bashlykov, Soumya Batra, Prajjwal Bhargava, Shruti Bhosale, et al. Llama 2: Open foundation and fine-tuned chat models. *arXiv preprint arXiv:2307.09288*, 2023. 1, 2
- [47] Zhengzhong Tu, Hossein Talebi, Han Zhang, Feng Yang, Peyman Milanfar, Alan Bovik, and Yinxiao Li. Maxvit: Multi-axis vision transformer. In *European conference on computer vision*, pages 459–479. Springer, 2022. 7
- [48] Aäron Van Den Oord, Nal Kalchbrenner, and Koray Kavukcuoglu. Pixel recurrent neural networks. In *ICML*, 2016. 1
- [49] Ashish Vaswani, Noam Shazeer, Niki Parmar, Jakob Uszkoreit, Llion Jones, Aidan N Gomez, Łukasz Kaiser, and Illia Polosukhin. Attention is all you need. In *NeurIPS*, 2017. 1
- [50] Haohan Wang, Songwei Ge, Zachary Lipton, and Eric P Xing. Learning robust global representations by penalizing local predictive power. In *Advances in Neural Information Processing Systems*, pages 10506–10518, 2019. 6
- [51] Peng Wang, Shijie Wang, Junyang Lin, Shuai Bai, Xiaohuan Zhou, Jingren Zhou, Xinggang Wang, and Chang Zhou. One-peace: Exploring one general representation model toward unlimited modalities. *arXiv preprint arXiv:2305.11172*, 2023. 2, 7
- [52] Wenhui Wang, Hangbo Bao, Li Dong, Johan Bjorck, Zhiliang Peng, Qiang Liu, Kriti Aggarwal, Owais Khan Mohammed, Saksham Singhal, Subhojit Som, et al. Image as a foreign language: BEiT pretraining for all vision and vision-language tasks. *arXiv preprint arXiv:2208.10442*, 2022. 2, 5, 7

- [53] Chen Wei, Haoqi Fan, Saining Xie, Chao-Yuan Wu, Alan Yuille, and Christoph Feichtenhofer. Masked feature prediction for self-supervised visual pre-training. *arXiv preprint arXiv:2112.09133*, 2021. [2](#), [5](#), [7](#)
- [54] Yixuan Wei, Han Hu, Zhenda Xie, Zheng Zhang, Yue Cao, Jianmin Bao, Dong Chen, and Baining Guo. Contrastive learning rivals masked image modeling in fine-tuning via feature distillation. *arXiv preprint arXiv:2205.14141*, 2022. [4](#), [5](#), [8](#)
- [55] Zhirong Wu, Yuanjun Xiong, Stella X Yu, and Dahua Lin. Unsupervised feature learning via non-parametric instance discrimination. In *CVPR*, 2018. [2](#)
- [56] Tete Xiao, Yingcheng Liu, Bolei Zhou, Yuning Jiang, and Jian Sun. Unified perceptual parsing for scene understanding. In *ECCV*, 2018. [6](#)
- [57] Zhenda Xie, Zheng Zhang, Yue Cao, Yutong Lin, Jianmin Bao, Zhuliang Yao, Qi Dai, and Han Hu. Simmim: A simple framework for masked image modeling. In *Proceedings of the IEEE/CVF Conference on Computer Vision and Pattern Recognition*, pages 9653–9663, 2022. [2](#)
- [58] Zhilin Yang, Zihang Dai, Yiming Yang, Jaime G. Carbonell, Ruslan Salakhutdinov, and Quoc V. Le. XLNet: Generalized autoregressive pretraining for language understanding. In *Advances in Neural Information Processing Systems 32: Annual Conference on Neural Information Processing Systems 2019, NeurIPS 2019, December 8-14, 2019, Vancouver, BC, Canada*, pages 5754–5764, 2019. [4](#)
- [59] Jiahui Yu, Zirui Wang, Vijay Vasudevan, Legg Yeung, Mojtaba Seyedhosseini, and Yonghui Wu. Coca: Contrastive captioners are image-text foundation models. *arXiv preprint arXiv:2205.01917*, 2022. [5](#)
- [60] Xiaohua Zhai, Alexander Kolesnikov, Neil Houlsby, and Lucas Beyer. Scaling vision transformers. In *Proceedings of the IEEE/CVF Conference on Computer Vision and Pattern Recognition*, pages 12104–12113, 2022. [2](#), [5](#)
- [61] Bolei Zhou, Hang Zhao, Xavier Puig, Tete Xiao, Sanja Fidler, Adela Barriuso, and Antonio Torralba. Semantic understanding of scenes through the ADE20K dataset. *Int. J. Comput. Vis.*, 127(3):302–321, 2019. [6](#)
- [62] Jinghao Zhou, Chen Wei, Huiyu Wang, Wei Shen, Cihang Xie, Alan Yuille, and Tao Kong. ibot: Image bert pre-training with online tokenizer. *arXiv preprint arXiv:2111.07832*, 2021. [5](#), [6](#), [7](#)